ELSEVIER

Carbohydrate Polymers 45 (2001) 373–383

Carbohydrate Polymers

www.elsevier.com/locate/carbpol

Hydrodynamic studies on chitosans in aqueous solution

H. Cölfen[a], G. Berth[b,*], H. Dautzenberg[a]

[a]*Max-Planck-Institut für Kolloid- und Grenzflächenforschung, Forschungscampus Golm, D-14476 Golm, Germany*
[b]*Institut für Organische Chemie und Strukturanalytik, Universität Potsdam, Am Neuen Palais 10, D-14469 Potsdam, Germany*

Received 20 December 1999; revised 9 June 2000; accepted 19 June 2000

Abstract

Three commercial chitosans with a degree of acetylation of 25–30% were studied by light scattering (static and dynamic), analytical ultracentrifugation (sedimentation velocity and sedimentation equilibrium), and capillary viscometry in 0.02 M acetate buffer/0.1 M NaCl, pH 4.5. The molecular masses obtained by sedimentation equilibrium measurements or sedimentation and diffusion coefficients according to the Svedberg equation agreed well or fairly well with those from static light scattering whereas the molecular masses calculated via the Scheraga–Mandelkern equation were found too low by almost 50%. The various Mark–Houwink type relationships suggested a nearly free-draining flexible worm-like chain. A prolate ellipsoid of revolution with an axial ratio $a/b \sim 25$ was shown to be a hydrodynamically equivalent body of the flexible worm-like chain that had been derived from static light scattering. The findings illustrate the fact that a hydrodynamically strongly asymmetric shape need not mean a strongly elongated shape of the molecules in reality.

Keywords: Chitosans; Molecular mass; Conformation; Light scattering; Ultracentrifugation; Viscosity; Diffusion; Sedimentation; Worm-like chain

1. Introduction

A knowledge of molecular parameters and conformation of polymeric materials in solution is useful for a better understanding of their behaviour in chemical and enzymatic reactions or intermolecular interactions between themselves or with other macromolecules, adsorption on surfaces, etc.

Because of the growing economic and academic interest in chitosan, we started studying chitosans in aqueous solution a few years ago. Static light scattering measurements (Berth, Dautzenberg & Peter, 1998; Berth & Dautzenberg, 2000) in acetate buffer, pH 4.5, (ionic strength $I \sim 0.12$ M) produced evidence for a single-stranded flexible chain conformation with a persistence length L_P of approximately 6 nm regardless of the degree of acetylation (DA) in a broad range of DAs (5–55%). Excluded volume effects as well as the polydispersity of the systems were taken into account in the calculations assuming a special logarithmic distribution function for the molecular weight and taking the number-average molecular weights M_n by membrane osmometry along with the weight-average molecular mass M_w by static light scattering (SLS) for the evaluation of the polydispersity M_w/M_n. Those average molecular weights (M_w, M_n) as well as the z-average radii of gyration ($R_{G,z}$) have been largely confirmed by recent high-performance size-exclusion chromatography experiments on TSK columns using multi-angle laser-light scattering detection (unpublished). Nevertheless, because of some severe problems in clarifying the solutions for subsequent light scattering analyses, there was a demand to check our results by another independent and absolute method. As such analytical ultracentrifugation (AUC) is most appropriate as it provides, like SLS, the weight-average molecular weight M_w (from sedimentation equilibrium) along with the second virial coefficient B.

Another way to obtain information on the molecular mass of a dissolved polymer is the combination of several hydrodynamic parameters. The most popular approach is to combine the sedimentation coefficient $s^0_{20,w}$ (from sedimentation velocity experiments in the analytical ultracentrifuge) and the translational diffusion coefficient $D^0_{20,w}$ (now-a-days mostly taken from dynamic light scattering measurements (DLS)) via the Svedberg equation (Svedberg & Pedersen, 1940). According to Scheraga and Mandelkern (1953), one can also combine $s^0_{20,w}$ or $D^0_{20,w}$ with the corresponding intrinsic viscosity $[\eta]$ of the system for an estimate of the molecular weight of a (monodisperse) polymeric solute using the β-parameter which, although being a hydrodynamic shape function, is highly insensitive to the molecular shape. Beyond the molecular mass, hydrodynamic parameters and functions contain information also on the

* Corresponding author. MPIKG Golm, D-14424 Potsdam, Germany.

0144-8617/01/$ - see front matter
PII: S0144-8617(00)00269-1

conformation of the solute. For example, according to the Stokes–Einstein equation (see, for example, Tanford, 1965), D^0 allows the calculation of the (average) hydrodynamic radius R_h which, combined with R_G, is useful for classifying macromolecules in terms of their 'gross' conformation (spheres, coils, and rods). A further quantity that is obtained from sedimentation velocity experiments in the analytical ultracentrifuge is k_s, the concentration dependence regression coefficient from a plot $(1/s^0_{20,w})$ versus concentration. k_s divided by the intrinsic viscosity $[\eta]$ gives the Wales–van Holde ratio (Wales & van Holde, 1954), which has also been used to estimate the 'gross' conformation of macromolecules in solution. In general, however, information on conformation is difficult to extract from hydrodynamic data because the experimentally observable global hydrodynamic behaviour of the molecules depends on two factors, which cannot be separated from each other without further information. These are the shape of the hydrodynamic particle and solvation (see, for example, Tanford, 1965; Yamakawa, 1971).

In previous studies on several complex polysaccharides, the combination of light scattering and hydrodynamic techniques as complementary methods revealed to be useful (reviewed in Berth & Dautzenberg, 1998).

For chitosan studies by simultaneous DLS/SLS (Wu, Zhou & Wang, 1995) on laboratory-made and low-acetylated samples (DA = 9%) led to a relationship between the diffusion constant $\bar{D}$ and the molecular mass M as $\bar{D} = \text{const.} \times M^{-0.665}$ so that the molecular weight distribution of any sample could be obtained by analysing the corresponding distribution of the diffusion coefficient. Weight-average molecular masses between $\sim 1 \times 10^5$ and $\sim 3.5 \times 10^5$ correlated reasonably with radii of gyration ($R_G = \text{const.} \times M_w^{0.64}$). Experimental R_G/R_h ratios between 1.7 and 2.0 have been consistent with a coil-like structure with excluded volume effects as well as a flexible worm-like chain model.

Based upon viscosity and DLS measurements (the latter conducted in a Malvern equipment at 90° only), Tsaih and Chen (1999) found that neither the ionic strength I ($0.01 < I < 0.20$) nor the pH (varied between pH 2.37 and 4.14) of the solvent substantially affected the gross conformation of chitosan (DA = 17%), which was claimed to be coil-like. The hydrodynamic volume was said to decrease with increasing pH or ionic strength. SLS measurements in the angular range between 30 and 140° were performed to determine M_w of the samples used. So it is difficult to understand why the authors did not make use of their $R_{G,z}$ data at all. $R_{G,z}$ along with M_w and the hydrodynamic radius R_h, respectively, would have been the most direct experimental approach to analyse the macromolecules conformation under varying conditions and easier to interpret than transport properties.

Hydrodynamic studies (Errington, Harding, Vårum & Illum, 1993) on two commercial chitosans of varying DA (11 and 48%, respectively) indicated significant differences in the individual sample behaviour. Parallel to capillary viscometry and dynamic light scattering measurements, sedimentation equilibrium and sedimentation velocity experiments were performed. Unusually low $D^0_{20,w}$ values were obtained from single-angle measurements at 90° in a Malvern instrument. Combined with the corresponding $s^0_{20,w}$ values via the Svedberg equation, these diffusion coefficients would lead to average molecular weights being 13–15 times as high as those from the sedimentation equilibrium analyses. Unfortunately, the authors did not comment on this part of their findings.

The present paper reports results from simultaneous static and dynamic light scattering (SLS/DLS) and analytical ultracentrifugation (sedimentation velocity and equilibrium experiments) on the three chitosans, which have already been the subject of previous investigations (Berth et al., 1998; Berth & Dautzenberg, 2000). Our studies aimed at obtaining a better understanding of chitosan behaviour in dilute (acidic) solutions as well as extending our experience in applying this approach to ionic polysaccharides.

2. Experimental

2.1. Samples and solution preparation

Three commercial chitosan samples with rather similar average DAs between 25 and 30% and referred to as Chit A, Chit B and Chit C were used. Some previously determined data (taken from Berth et al., 1998; Berth & Dautzenberg, 2000) are listed in Table 1.

The samples were dissolved at room temperature in 0.02 M acetate buffer/0.1 M NaCl, pH 4.5 ($\rho^{20°C} = 1.00343$ g/ml, $\eta^{22°C} = 0.971$ cP) overnight under slight shaking (some 'flocks' remained). Then the solutions were ultracentrifuged for 90 min at 40,000 rpm and 25°C using a Beckman preparative ultracentrifuge L-70 (Beckman Instruments, Palo Alto CA) and a fixed-angle rotor Ti 70.1. The supernatant was filtered through membrane filters in order of decreasing pore size (8.0, 5.0, 1.2, 0.8, 0.45 (0.2) μm twice at each stage). The concentration was checked refractometrically ($\delta n/\delta c = 0.203$ ml/g). Solutions prepared in this way

Table 1
Intrinsic viscosities (Berth et al., 1998) and degrees of acetylation (Berth & Dautzenberg, 2000) of the samples used in this study

Sample	Average degree of acetylation DA (%)	Intrinsic viscosity $[\eta]$ (ml/g)
Chitosan A	27–31[a]	333
Chitosan B	22–27[a] 22.5[b]	150
Chitosan C	25–31[a]	650

[a] By colloid titration.
[b] By potentiometric titration.

with concentrations ranging from 0.2 to 2.5 mg/ml were taken for the light scattering (DLS/SLS) and AUC experiments.

For the determination of the partial specific volume $\bar{v}$, a weighed amount of chitosan (~2 mg/ml) was suspended in the buffer above and dialysed (cut-off of the membrane: 1 kDa) against an excess of solvent at least for 24 h. The concentration after dialysis was determined refractometrically (ScanRef, Nanofilm Technologie GmbH, Germany) with $\delta n/\delta c = 0.203$ ml/g at 633 nm. Afterwards, the densities on a dilution series of this stock solution were measured in an DMA 602 density measuring instrument (AP Paar Chempro, Austria) at 20°C.

2.2. Light scattering measurements

Light scattering measurements were carried out in an ALV goniometer with ALV-5000 digital time correlator (ALV Langen, Germany) between 30 and 150° (in intervals of 5°) at the wavelength $\lambda_0 = 532$ nm (400 mW laser, Spectra Physics, USA) and 22°C. At least three runs per 30 s were carried out to calculate the average scattering intensities at each angle. The Zimm procedure was used to derive M_w, $R_{G,z}$, and B in the common way. 'Dynamic Zimm plots' were constructed in analogy to derive D^0, the diffusion coefficient extrapolated to zero angle and zero concentration. The diffusion coefficient D at any single concentration and angle of observation was obtained by a cumulant fit of second order. The diffusion coefficients D^0 were corrected to the standard conditions at 20°C using the formula given by Tanford (1965, p. 357).

2.3. Analytical ultracentrifugation experiments

A Beckman XL-I analytical ultracentrifuge (Beckman Instruments, Palo Alto, CA) was used for all experiments applying the on-line Rayleigh interferometer. Sedimentation velocity experiments were performed at 60 000 rpm whereas sedimentation equilibrium experiments were done at 8000, 12 000 and 18 000 rpm. All experiments were performed at 25°C in self-made titanium 12-mm double sector centrepieces. The sedimentation coefficients were determined via the boundary movement and corrected to standard conditions at 20°C with the formula given by Tanford (1965). Sedimentation equilibrium experiments were evaluated using the MSTAR algorithms (Cölfen & Harding, 1997).

3. Results and discussion

3.1. Simultaneous static and dynamic light scattering measurements

Results by simultaneous SLS and DLS are listed in Table 2 along with previous data from static light scattering alone (Berth et al., 1998) as well as HPSEC/MALLS. Comparison of the 'old' and 're-estimated' values shows good or satisfactory agreement for M_w and $R_{G,z}$ (or at least the M_w–$R_{G,z}$ relation) for all three samples thus illustrating the feasibility of light scattering experiments under the chosen conditions. The B values obtained for the same sample vary by a factor of up to 2.5 and, although being in the theoretically anticipated order of magnitude, they have poor reproducibility. Zimm plots for Chit B are shown in Fig. 1a and b. The 'static Zimm plot' is reminiscent of previously presented graphs (Berth et al., 1998). The 'dynamic Zimm plot' in Fig. 1b shows only a weak dependence of D on concentration and angle of observation along with relatively strong fluctuations of the individual points.

Despite somewhat different solvent compositions and DAs, the pairs of $R_{G,z}$ and M_w in Table 2 have already been shown to fit reasonably well the data sets published by Wu and Wang in 1994 (see Berth et al., 1998; Fig. 8). So do now our pairs of R_h and M_w. With $D^0 \sim M^{-0.67}$ or

Table 2
Results by static and dynamic light scattering

Sample	Molecular mass M_w (g/mol)	z-Average root mean square radius of gyration R_G (nm)	Second virial coefficient B_{SLS} (ml mol g^{-2})	Translatorial diffusion coefficient $D^0_{20,w}$ (cm^2 s^{-1})	Hydrodynamic radius R_h (nm) via Stokes–Einstein	R_G/R_h	Method/equipment
Chitosan A	63,800	33	3.55×10^{-3}				SLS (Sofica)[a]
	72,000	35					HPSEC/MALLS[b]
	64,900	35	1.43×10^{-3}	14.5×10^{-8}	15.3	2.3	SLS/DLS (ALV)[c]
Chitosan B	39,300	31.4	3.88×10^{-3}				SLS (Sofica)[a]
	44,100	28	2.41×10^{-3}	19.8×10^{-8}	11.2	2.6	SLS/DLS (ALV)[c]
Chitosan C	147,000	59.3	6.76×10^{-3}				SLS (Sofica)[a]
	134,000	46					HPSEC/MALLS[b]
	180,000	62	4.03×10^{-3}	9.1×10^{-8}	24.5	2.3	SLS/DLS (ALV)[c]

[a] Berth et al. (1998).
[b] Unpublished.
[c] This paper.

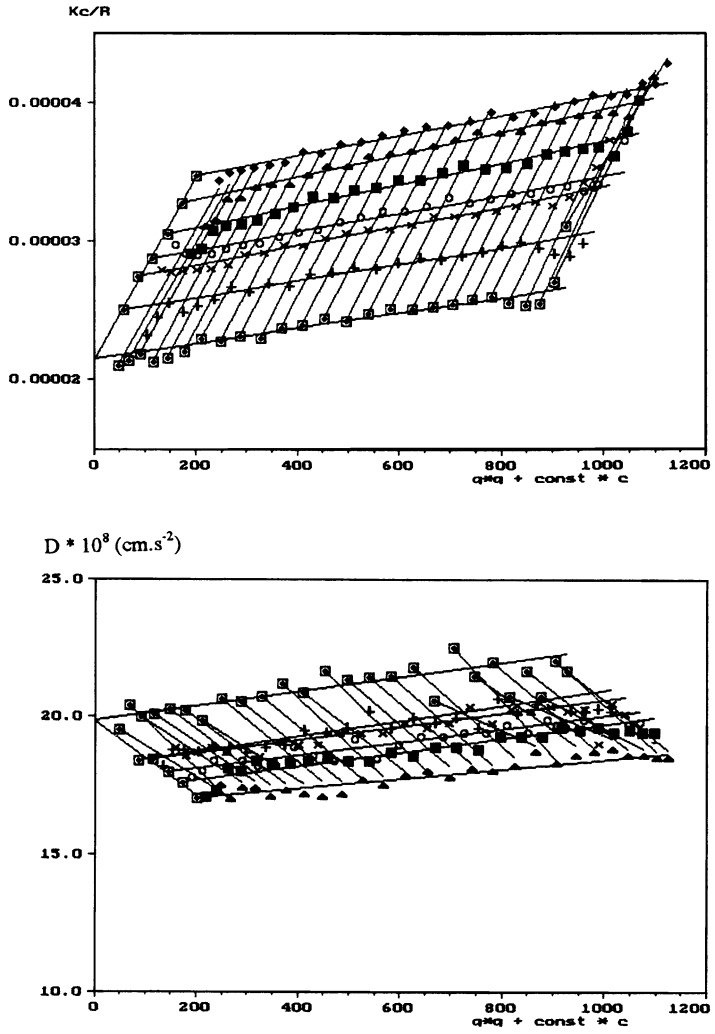

Fig. 1. Simultaneous static and dynamic light scattering on Chit B in acetate buffer, pH 4.5; ionic strength ~0.12 M. (a) 'Static Zimm plot'; $M_W = 44,100$ g/mol; $R_{G,z} = 28$ nm; $B = 2.4 \times 10^{-3}$ ml mol g^{-2}. (b) 'Dynamic Zimm plot'; $D^0 = 19.8 \times 10^{-8}$ cm^{2}s^{-1}; $R_h = 12$ nm (via Stokes–Einstein equation).

alternatively $R_h \sim M^{0.67}$ (since $D^0 \sim 1/R_h$), our findings follow closely the relationship derived by those authors. R_G/R_h data are given in Table 2. The values of 2.3 (Chit A and Chit B) and 2.6 (Chit C) move around the anticipated value for coil like structures ($R_G/R_h = 1.75$) or flexible worm-like chains and still seem acceptable since no correction for polydispersity was made. Altogether these data are consistent with the previously derived worm-like chain model (Berth et al., 1998). Seen in the context of our previously reported $[\eta]$–M_w relationship (Berth et al., 1998, Fig. 7), the following consideration, which is based upon generally accepted conceptions, might be useful: With $[\eta] \sim (R_G^3/M)$ and $R_G \sim R_h \sim M^{0.67}$, one obtains $[\eta] \sim (M^{2.01}/M)$ which means $[\eta] \sim M^1$. This corresponds largely to what has been presented for the low-molecular weight region below about 200 000 g/mol. Obviously our results from SLS/DLS and viscosity measurements are consistent.

The significantly lower diffusion coefficients reported by Errington et al. (1993) could not be confirmed whereas their $[\eta]$–M_w data pairs (except KN50-1) are not too different from ours. So the comparison of data suggests to assume that their D^0 values were likely affected by big particulate matter because of an inefficient clarification procedure. Such particles dominate the scattering behaviour but do not produce discernible effects on viscosity or sedimentation measurements.

3.2. Sedimentation velocity measurements

First, the homogeneity of the chitosans was investigated. All samples sedimented as single boundaries. A more detailed analysis of the apparent sedimentation coefficient distribution $g(s^*)$ reveals that at least three Gaussian curves were needed in order to fit the experimental curves satisfactorily (Fig. 2) suggesting *heterogeneous* samples. In principle, the term heterogeneity may cover (i) the ordinary molecular weight distribution of any chitosan sample ('polydispersity'), (ii) variations of the conformation of

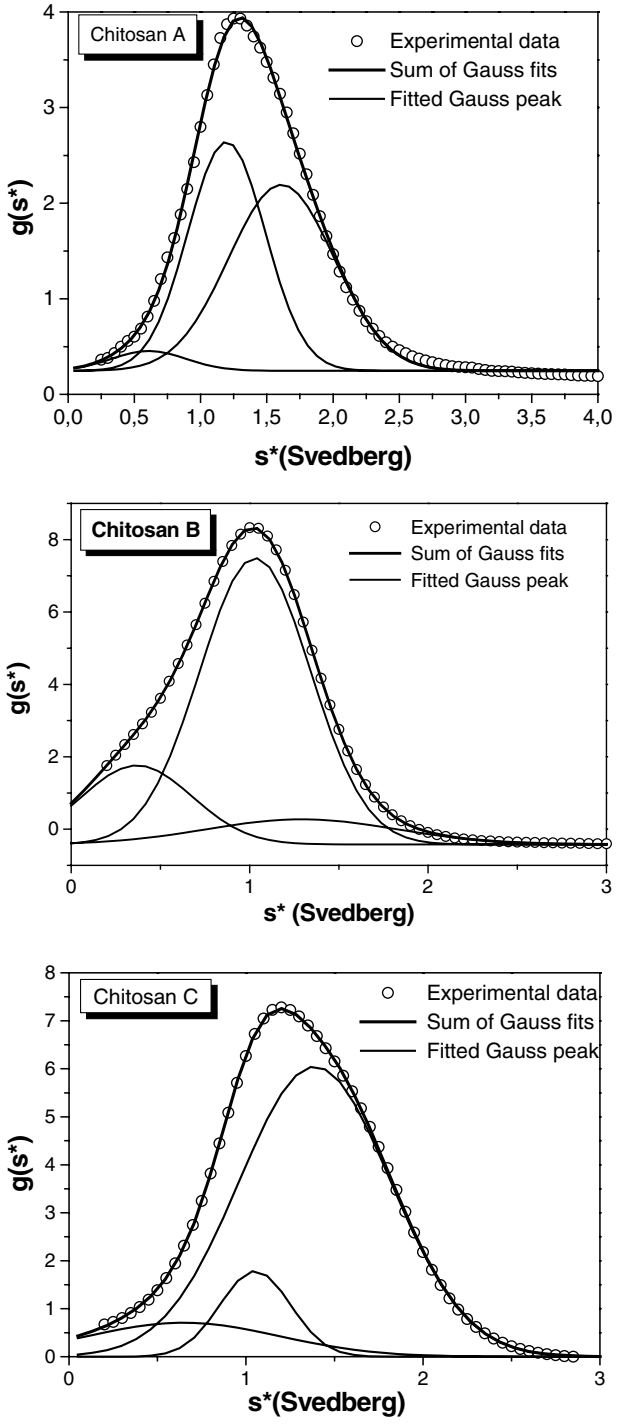

Fig. 2. Apparent sedimentation coefficient distributions $g(s^*)$ of chitosans A (0.8 mg/ml), B (2.30 mg/ml) and C (1.94 mg/ml) fitted to multiple Gauss peaks.

the dissolved species due to partial aggregation or branching and (iii) density distributions due to variations of the DA within the population. Separate studies on the distribution of the DA across the molecular weight distribution (Berth & Dautzenberg, 2000) have indicated chemically largely homogeneous samples (apart from a few percent of low-molecular weight but high acetylated material) so that $g(s^*)$ is supposed to result primarily from polydispersity.

Fig. 3 exhibits the reciprocal sedimentation coefficients $1/s^0_{20,w}$ as function of the polymer concentration. A critical inspection shows the individual differences among the three samples to be rather small. A linear extrapolation to zero concentration provides the $s^0_{20,w}$ and k_s values collected in Table 3. Due to the relatively large errors of the individual data points, particularly k_s has to be considered with reservation.

In the case of Chit C both $s^0_{20,w}$ and k_s depend strongly on whether all data pairs are taken into account (values in brackets) or only those up to a concentration of ~1.1 mg/ml. The downward curvature for the higher concentrations might indicate some aggregation so that it seemed reasonable to neglect these points. That is why $s^0_{20,w} = 1.97$ S and $k_s = 166$ ml/g resulting from the dash-dot line in Fig. 3 is given preference.

According to Lavrenko, Linow and Görnitz (1992), there is a relationship between $s^0_{20,w}$ and k_s. Calculating k_s from $s^0_{20,w}$ via their empirically found power function $k_s = Y(s^0_{20,w} \times 10^{13})^{\kappa}$ and using also their values for chitosan as $Y = 52$ and $\kappa = 2.5$, we obtained. $k_s = 127$ for Chit A, $k_s = 110$ for Chit B, and $k_s = 283$ for Chit C (Table 3). Whereas the differences for Chit B and Chit C are considerable, the value for Chit A agrees well with that from our experiments.

The order of magnitude of $s^0_{20,w}$ for all three chitosans compares well to sedimentation coefficients measured elsewhere (Errington et al., 1993) for chitosans from a wide range of degrees of acetylation and molecular masses despite a somewhat different buffer composition. Combined with the standardised $D^0_{20,w}$ from dynamic light scattering according to the Svedberg equation (Svedberg & Pedersen, 1940):

$$M_w = \frac{s^0_{20,w} R T}{D^0_{20,w}(1 - \bar{v})\rho_0)}, \quad (1)$$

the average molecular masses M_w in Table 3 were obtained. R stands for the universal gas constant ($R = 8.3166 \times 10^7$ g cm^2 s^{-2} K^{-1} mol^{-1}) and T for the temperature in Kelvin. $\bar{v}$ is the partial specific volume (Table 3) and ρ_0 is the density of the solvent.

The molecular masses in column 7 follow the expected order but the agreement with the SLS data is good only for Chit B. The other two samples seem underestimated by up to 25% compared with the SLS results. However, these deviations do not essentially exceed those from different SLS experiments on the same matter (SLS standing alone or HPSEC/MALLS). In view of the particular experimental difficulties produced by the polysaccharide itself, the agreement between AUC/ DLS data on the one hand and SLS on the other hand data is taken as acceptable. This is even more so as molecular masses determined via the Svedberg equation are generally known to exhibit higher errors than those derived by

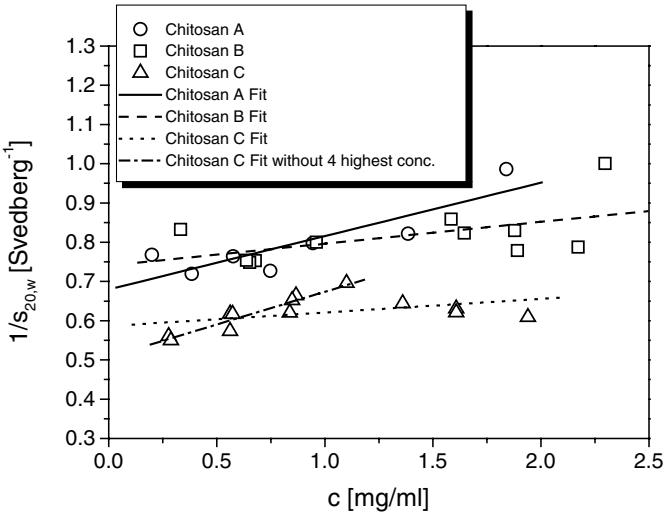

Fig. 3. Reciprocal sedimentation coefficients ($1/s_{20,w}$) versus concentration for Chit A, B and C.

absolute techniques such as SLS and sedimentation equilibrium (see below).

In addition to the Svedberg equation, the Scheraga–Mandelkern function β (Scheraga & Mandelkern, 1953)

$$\beta = \frac{N_A s^0_{20,w}[\eta]^{1/3}\eta_0}{M^{2/3}(1-\bar{\nu}\rho_0)100^{1/3}} \quad (2)$$

can be used for an estimation of M from $s^0_{20,w}$ and [η], respectively, from $D^0_{20,w}$ and [η]. η_0 is the viscosity of the solvent (in P) and N_A the Avogadro's number. The limits of β are 2.12 to 2.50×10^6 for solid spheres, flexible coils, oblate ellipsoids of any axial ratio and prolate ellipsoids for axial ratios up to $a/b = 13$ (Tanford, 1965, p. 399). For prolate ellipsoids of revolution β is proportional to $(\nu^{1/3}/P)$ with ν being the Simha factor (Simha, 1940) and P the Perrin factor (Perrin, 1936). Having interpreted the hydrodynamic data by means of the 'whole body approach', we found a prolate ellipsoid with an axial ratio $a/b = 25$ to appropriately describe our results (see the paragraph 'Wales–van Holde ratio R' later on). Then β becomes $\beta = 2.71\times10^6$ and leads to the molecular masses in Table 3. Again, the values are considerably lower than those obtained by light scattering and even significantly below those derived via the Svedberg equation. This discrepancy might be an effect of partial draining of the worm-like chain structure of chitosans, which is known to strongly reduce [η].

3.3. Intrinsic viscosities

In the framework of the Kirkwood–Riseman theory, the extent of draining can be estimated from viscosity data by comparing the actually measured intrinsic viscosity with the theoretical value for the non-draining case (NDC). The latter is obtained according to

$$[\eta] = 6^{3/2}\Phi_0\frac{\langle R^2_G\rangle^{3/2}}{M} \quad (3)$$

Φ_0 varies with the draining parameter 'X', which can be expressed as

$$\Phi_0(X) = (\pi/6)^{3/2}N_A[XF(X)]$$

with $X = \infty$ and $\Phi_0 = 2.87\times10^{23}$ for the non-draining case and $X = 0$ for the free-draining case. $XF(X)$ is a decreasing function of X (see the Table on p. 269 in Yamakawa, 1971). Having performed the calculations,

Table 3
Sedimentation coefficients ($s^0_{20,w}$), concentration dependence regression coefficients (k_s), partial specific volume ($\bar{\nu}$) and molecular masses (M_w) by hydrodynamics

Sample	$s^0_{20,w}$ (S)	k_s (ml/g)	k_s[a] (ml/g)	$R = k_s/[\eta]$	$\bar{\nu}$ (ml/g)	M_w (g/mol)	
						via Svedberg equation	via Scheraga–Mandelkern
Chit A	1.43 ± 0.05	140 ± 30	127	0.42/0.38[a]	0.542	52,300	33,500
Chit B	1.35 ± 0.082	56 ± 29	110	0.37/0.73[a]	0.551	44,200	21,300
Chit C	(1.72 ± 0.06)	(30 ± 20)	(199)	(0.05)	0.544	(98,500)	(62,300)
	1.97 ± 0.06[b]	166 ± 23[b]	283	0.26/0.44[a]		110,000	76,300

[a] Calculated according to Lavrenko et al. (1992).
[b] Neglecting the data points at higher concentrations.

Table 4
Estimate of the extent of draining

Sample	M[a] (g/mol)	R_G[b] (nm)	$[\eta]_{exp}$[a] (ml/g)	$[\eta]_{NDC}$ (ml/g)	$[\eta]_{exp}/[\eta]_{NDC} = \Phi_0(X)/\Phi_0(\infty)$	X[c]
Chit A	64,000	23	333	834	~0.4	~1
Chit B	39,300	22	150	1483	~0.1	~0.2
Chit C	147,000	37	650	1453	~0.4	~1

[a] See Tables 1 and 2.
[b] Corrected to the weight-average value (Berth et al., 1998).
[c] Taken from Yamakawa (1971, p. 269).

the values in Table 4 were obtained. As can be seen, X is found very small indicating a situation near the *free-draining* case. (X would be even smaller if R_G was related to Θ conditions.) This is consistent with the high exponent in the $[\eta]$–M_w relationship found by our experiments and elsewhere (e.g. Ottøy, Vårum, Christensen, Anthonsen & Smidsrød, 1996).

3.4. Mark–Houwink–Kuhn–Sakurada (MHKS) coefficients

According to the relations $[\eta] = KM^a$, $s^0_{20,w} = K^I M^b$, $D^0_{20,w} = K^{II} M^{-\epsilon}$ and $R_g = K^{III} M^c$, we have obtained the scaling exponents given in Table 5.

All exponents are consistent with a random coil model rather than a rigid rod one. Consequently, the nearly free-draining flexible worm-like chain seems an appropriate model. The specified values from this study agree well with those given for carboxymethyl-chitin (CMCh), which was also discussed to behave like a worm-like chain (Pavlov, Korneeva, Harding & Vichoreva, 1998).

The reciprocal relationships among the scaling exponents are as follows: The sedimentation coefficient s is proportional to M by $s^0_{20,w} = kM^b$. $s^0_{20,w}$ is also related to the hydrodynamic radius R_h according to $s^0_{20,w} \sim (M/R_h)$, where, in our specified case, R_h has been derived to depend on M according to $R_h \sim M^{0.67}$ (see above). Having substituted R_h by $M^{0.67}$, we obtain $s^0_{20,w} \sim M^{0.33}$. This is what would be predictable from our DLS measurements. Consequently, the sedimentation velocity method is much less sensitive to indicate changes in M than, e.g. measurements of D^0 or $[\eta]$. The molecular weight dependence actually measured is even below the predicted one no matter on which of the molecular masses in Tables 2 and 3 calculations are based. A representative value of $b \approx 0.24$ is given in Table 5.

Table 5
Compilation of the scaling exponents of the Mark–Houwink type plots

Sample or model	a	b	ϵ	c
Chitosan	~1	0.24	0.67	0.67
Carboxymethyl-chitin[a]	0.94	0.39	0.60	n.d.
Rigid rod	1.8	0.15	0.85	1
Random coil	0.5–0.8	0.4–0.5	0.5–0.6	0.5–0.6

[a] Values taken from Pavlov et al. (1998).

The weak effect of M on $s^0_{20,w}$ in our experiments agrees widely with results reported by Errington et al. (1993). For changes in M_w (from sedimentation equilibrium) by a factor of 5.6 they obtained changes in $s^0_{20,w}$ by a factor of ~1.1.

One of the consequences of that discussion is the dominance of D^0 in calculating M_w from $s^0_{20,w}$. This means the applicability of the Svedberg equation for chitosans depends to a great extent on the reliability of the available D^0 data. In any case, the resultant M_w must be considered with reservation and the method cannot replace absolute techniques such as SLS and sedimentation equilibrium experiments.

3.5. Sedimentation equilibrium measurements

Sedimentation equilibrium experiments were performed only on Chitosan A. To check a possible speed dependence of the apparent weight average molar mass $M_{w,app}$ caused by the polydispersity of the material, measurements were made at the speeds of 8000, 12 000 and 18 000 rpm. Results are shown in Fig. 4.

Obviously, there is no pronounced speed dependence of $M_{w,app}$ so that the data points for all speeds could be combined. Linear regression of $1/M_{w,app}$ vs. c yielded M_w = 70 300 g/mol discarding the data points for the highest concentration and the points for 8000 and 12 000 rpm for the lowest concentration. The second virial coefficient B was determined from the slope of the regression line to be 1.12×10^{-3} ml mol g^{-2}. The molecular mass is in really good agreement with the values in Table 2 whereas the virial coefficient is somewhat lower than even the lowest one found by static light scattering.

3.6. Whole body approaches

Particularly in the ultracentrifuge community a 'whole-body approach' has become common practice in order to describe the hydrodynamics of macromolecules.

3.6.1. Wales van Holde ratio R

Dividing k_s from sedimentation velocity experiments by the intrinsic viscosity $[\eta]$ to give the Wales–van Holde ratio R (Wales & van Holde, 1954) provides a sensitive and

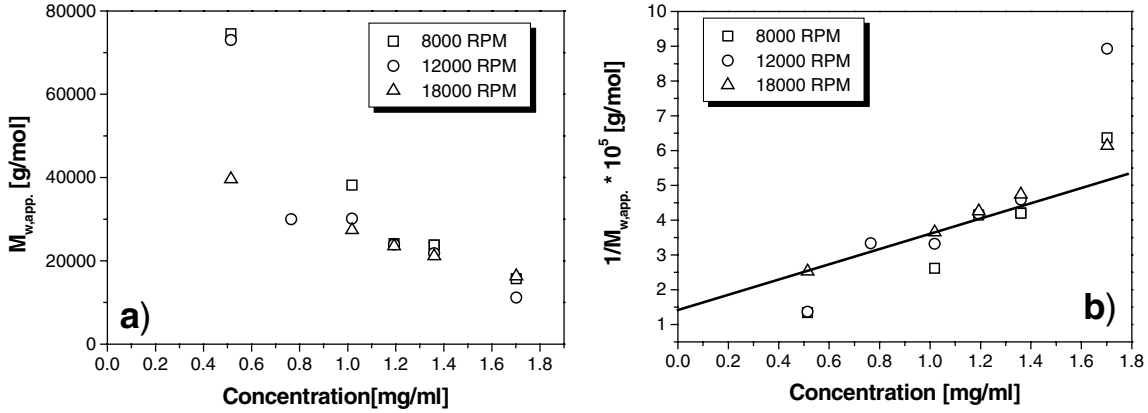

Fig. 4. (a) Concentration dependence of $M_{w,app}$ for Chitosan A and (b) of $1/M_{w,app}$ at three different speeds.

hydration-independent function for small axial ratios (Harding, 1995) and at least an estimate of the axial ratio of elongated particles. Under the assumption that

1. the migration velocity of particles with respect to the solvent is independent of c at infinitely low c;
2. no interactions between the solute or additional components take place;
3. $\bar{v} = 1/\rho_{solute}$;
4. the system is incompressible.

Rowe (1977) derived the expression

$$k_s = 2\bar{v}\left[\frac{v_s}{\bar{v}} + \left(\frac{f}{f_0}\right)^3\right] \tag{4}$$

with $\bar{v}$ being the partial specific volume of the solute and v_s the total specific volume of the solute where solvation is included. f/f_0 describes the deviation of the frictional coefficient from that of a sphere with a partial specific density $\bar{\rho} = 1/\bar{v}$ and contains both the contribution of shape anisotropy of the particle and solvation which is

$$\frac{f}{f_0} = P\left(\frac{v_s}{\bar{v}}\right)^{1/3} \tag{5}$$

with P being the Perrin factor.

With a possible exception of point 2, the assumptions in the list above are fulfilled for the chitosan system.

The intrinsic viscosity can be expressed by

$$[\eta] = \nu v_s \tag{6}$$

with ν being the Simha factor (see, for example, Tanford, 1965) which is tabulated for various axial ratios (see, for example, Harding, 1995). Substituting k_s and $[\eta]$ by Eqs. (4) and (6), respectively, one obtains

$$R = \frac{k_s}{[\eta]} = \frac{2\bar{v}}{\nu v_s}\left[\frac{v_s}{\bar{v}} + \left(\frac{f}{f_0}\right)^3\right] \tag{7}$$

From Eqs. (5) and (7), a simple relation between R, P and ν is obtained:

$$R = \frac{2}{\nu}[1 + P^3] \tag{8}$$

To calculate the axial ratio (a/b) of a prolate ellipsoid of revolution via the determined R-values, inversion formulae had to be applied as discussed in Harding and Cölfen (1995). The routine ELLIPS1 (Harding, Horton & Cölfen, 1997a) was used for that purpose. Our R values ranged from 0.41 $\{(a/b)_{prolate} = 24\}$ for Chit A, 0.37 $\{(a/b)_{prolate} = 30\}$ for Chit B, to $R = 0.26$ or $(a/b)_{prolate} = 74$ for Chit C. Each of these values is clearly lower than that of $R = 1.3$–0.6 reported by Pavlov and Selyunin (1986), for chitosans with M between 14 000 and 172 000 g/mol. At a glance, the hydrodynamically strongly elongated shape seemed to be in contradiction with the worm-like chain model in the preceding paragraph. The problem which we were faced with at this point of discussion was how to interpret these findings. The details of our approach are as follows.

Having determined $a/b = \tau$ from R, one obtains v_s which is described by

$$v_s = \frac{V_E N_A}{M} \tag{9}$$

with V_E being volume of the ellipsoid of revolution, N_A the Avogadro's number, and M the molecular mass.

The volume of a single ellipsoid of revolution is defined by $V_E = (4\pi/3)\tau b^3$. Having replaced V_E by this expression, Eq. (10) follows from Eq. (9):

$$b = \left(\frac{3v_s M}{4\pi N_A \tau}\right)^{1/3} \tag{10}$$

The radius of gyration of such an ellipsoid of revolution is obtained according to

$$R_G^2 = \tfrac{1}{5}b^2(2 + \tau^2) \tag{11}$$

(see, for example, Elias, 1990). Having a value for R_G, a good estimate of the Kuhn segment length L_K can be made

by using the relation for Gaussian coils:

$$R_G^2 = \frac{L_K L}{6} \quad (12)$$

with L being the contour length.

From the experimentally measured [η] along with ν (from τ via R) one can calculate v_s.

Furthermore, the effect of the molecular mass on the relationship between axial ratio τ and the Simha factor ν can be estimated. For large axial ratios and with $R_G \sim M^c$, one can write

$$R_G \sim b\tau \sim \left(\frac{Mv_s}{\tau}\right)^{1/3} \tau \sim M^{1/3} v_s^{1/3} \tau^{2/3} \sim M^c$$

making use of the Eqs. (11) and (10). From that follows

$$\tau^2 v_s \sim [\eta] \frac{\tau^2}{\nu} \sim M^{3c-1}$$

because of Eq. (6)). With $[\eta] \sim M^a$, one obtains

$$\frac{\tau^2}{\nu} \sim \frac{M^{3c-1}}{M^a} \sim M^{3c-a-1}.$$

Applied to our chitosan samples with $R_G \sim M^{0.67}$ and $[\eta] \sim M^1$ (Table 5), one obtains $(\tau^2/\nu) \sim M^{3\cdot 0.67-1-1} \cong M^0$. This means the Wales–van Holde ratio R is predicted not to depend on the molecular mass M ($R \sim M^0$). This is not what was actually measured (Table 3, column 5) but we have already stated our reservation regarding the reliability of the individual k_s data. Amongst them, the data for Chit A seem most reasonable. At the moment, we can only speculate about where that inconsistency might come from. Since the light scattering experiments on the same samples in the same solvent after the same clarification procedure yielded relatively reliable data, one can scarcely operate with the poor quality of the industrial samples or their generally unclear solubility status. The most obvious difference between our light scattering and ultracentrifugation experiments is that the AUC measurements covered a distinctly higher range of polymer concentrations than the SLS studies normally did. (Higher concentrations in the AUC were desired to increase precision but were not advantageous in the light scattering experiments.) For all the reasons given, we have taken a unique $R = 0.4$ and hence $a/b = 25$ for all further calculations according to the Eqs. (6) and (9)–(12). Then, based on $[\eta] = 650$ ml/g and $R = 0.4$, $k_s = 260$ ml/g comes out for Chit C in good accordance with the value predicted by Lavrenko's approach (Table 3).

Results of our calculations are collected in Table 6. A unique mass per unit length $M_L = 350\text{g mol}^{-1}\text{nm}^{-1}$ was taken to calculate the weight-average contour length L_w in column 3 by $L_W = (M_W/M_L)$. $R_{G,z}$ was corrected to the corresponding weight-average value by means of $(R_{G,z}^2/R_{G,w}^2) = (M_w/M_n)$ for the sake of comparison (this relation is valid for the logarithmic distribution function applied previously, see Berth, Dautzenberg and Peter (1997)). Comparing now the L_K values originating from the hydrodynamic experiments with those measured by static light scattering, one will notice a relatively good agreement with $L_K \sim 13$ nm (on average) just as it was discussed before. The individual deviations seem still tolerable if we take the experimental errors of each of the methods into account and accept the assumptions that had to be made.

Table 6
Results of calculations aimed at the interpretation of data in terms of conformation)

	Chit A	Chit B	Chit C
M_w (g/mol)[a]	64,000	39,300	147,000
L_w (nm)	183	112	420
[η] (ml/g)[a]	333	150	650
$R_{G,z}$ (nm)[a]	33.0	31.4	59.3
M_w/M_n[a]	2.05	1.92	2.56
$R_{G,w}$ (nm)	23.0	22.7	37.1
k_s (ml/g)	140	56	166
R[b]	0.4	0.4	0.4
$a/b = \tau$	25	25	25
P	2.17	2.17	2.17
f/f_0			
From P and v_s	4.8	3.7	6.0
From $s^0_{20,w}$	7.5	5.6	9.5
From $D^0_{20,w}$	6.2	5.6	7.5
ν	55.9	55.9	55.9
v_s (ml/g)	6.0	2.7	11.6
b (nm)	1.83	1.19	3.00
R_G (nm)	20.5	13.3	33.6
L_K^{GC} (nm)	13.8	9.5	16.1
L_K (nm) SLS[a]	13.0	25.0	12.0
w (g/g)	5.5	2.1	11.1

[a] Taken from Berth et al. (1998).
[b] Taken uniquely for reasons given in the text.

Having determined a value for v_s, the mass w of the total amount of 'entrapped' solvent (chemically and physically bound) can be calculated according to

$$v_s = \bar{v} + w/\rho_0 \quad (13)$$

with $\rho_0 = 1.00343$ ml/g for the solvent density. w is given in gram solvent per gram polymer. The results in Table 6 show increasing amounts of bound water with increasing molecular masses. This agrees with what would be anticipated from our principal understanding of solvation. Compared with the value $w \sim 50$ g/g for carrageenan ($M_w \approx 300\,000$ g/mol) reported by Harding, Day, Dhami and Lowe (1997b), the amount of entrapped water is relatively small.

3.6.2. Perrin function and frictional coefficient

For reasons of completeness, we have also listed the corresponding Perrin functions P and frictional coefficients f/f_0 because these quantities are of general interest in the field of hydrodynamics. P is obtainable according to Eq. (8) from R and ν and was calculated to be $P = 2.17$ for the chitosan samples in this study. f/f_0 can be calculated if P

and v_s are known. f/f_0 can also be determined via the directly measurable quantities $s^0_{20,w}$ together with a derivative of the Svedberg equation

$$\left(\frac{f}{f_0}\right) = \frac{M(1-\bar{v}\rho_0)}{N_A 6\pi\eta s^0_{20,w}}\left(\frac{4\pi N_A}{3\bar{v}M}\right)^{1/3} \quad (14)$$

or via $D^0_{20,w}$ using

$$\left(\frac{f}{f_0}\right) = \frac{kT}{6\pi\eta}\left(\frac{4\pi N_A}{3\bar{v}M}\right)^{1/3}\frac{1}{D^0_{20,w}} \quad (15)$$

with k being the Boltzman's constant and η the viscosity of the solvent.

Table 6 presents the values from all three procedures. They differ but show the expected order with the lowest value for the low-molecular weight sample etc. The value for Chit C is fairly close to $f/f_0 \sim 7.6$ reported for the system κ-carrageenan/water (Harding et al., 1997b) with $R = 0.9$ and $(a/b) = 15$. In the case of carrageenan, these data have been attributed to the highly expanded and rigid chain conformation. In our view, it would make sense to underpin such conclusions by means of the radius of gyration by light scattering (see, for example, Vanneste, Slootmaekers & Reynaers, 1996) as above in order to overcome all ambiguity of an interpretation that is based solely on hydrodynamic data.

3.6.3. Π-function

Another sensitive shape function for the determination of the axial ratio of prolate ellipsoids is the Π-function (Harding, 1981) which has the form $\Pi = (2BM/[\eta])$ under the assumption that the effect of charges can be neglected because of a sufficient ionic strength ($I = 0.12$ M in these experiments). Calculating Π and using the routine ELLIPS1 (Harding et al., 1997a), we got axial ratios (a/b) of a prolate ellipsoid ranging from 2 to 80 with the majority of values between $\Pi = 1$ and $2\{(a/b)_{\text{prolate}} = 29\text{–}9\}$ depending on the source of M_w and B and reflecting the differences in the molar masses (about 20%) and primarily those in B (Table 1). As the scattering of these values is so high, the data cannot be taken as reliable measure of configuration here.

3.6.4. Triaxial ellipsoids

It is possible to calculate the axial ratios of triaxial ellipsoids with a graphical intersection approach by combining the reduced radius of gyration function G with Π (Harding, 1995). Although it might seem unwise to continue with those questionable Π values, we have applied the routine for reason of completeness. However, the large errors in Π were only amplified so that this approach did not provide any useful information.

4. Conclusions

The molecular weight of Chit A from sedimentation equilibrium experiments was found in good agreement with that determined by static light scattering. Fairly good agreement between molmasses by light scattering and ultracentrifugation was achieved for all three samples when sedimentation and diffusion coefficients were combined according to the Svedberg equation. The quality of results was primarily limited by the experimental errors linked with each of the techniques. The approach proposed by Scheraga & Mandelkern was found to completely fail.

The viscosity and light scattering data altogether are fully consistent with the model of a nearly free-draining wormlike chain. The hydrodynamic behaviour is equivalently represented by a prolate ellipsoid of revolution of extremely high asymmetry (whole-body approach). A highly asymmetric molecular shape is, however, in clear contradiction to the found exponents in the M-dependence of $[\eta]$ and R_G. Following the algorithm proposed, it has been shown that the hydrodynamic behaviour of a nearly free-draining flexible wormlike chain is equivalently represented by the big axial ratio for a prolate type ellipsoid of revolution and reverse. In other words, a *hydrodynamically* strongly asymmetric shape does not necessarily mean a strongly asymmetric real molecular particle. Then the calculated amount of entrapped water is strongly underestimated. These messages are not new (see, e.g., Tanford, 1965). The example given is hoped to illustrate that it makes sense to combine results from hydrodynamics with those by light scattering. The latter is the only method to provide the radius of gyration free of any assumptions.

Also the collection of Mark–Houwink–Kuhn–Sakurada type equations offers a real chance to get reasonable information on the chain conformation.

The fact that data from different laboratories and measured on samples of strongly varying degree of acetylation were found to suit each other satisfactorily well under all sorts of aspects (Errington et al., 1993; Wu et al., 1995; Ottøy et al., 1996; Berth et al., 1998; this paper) is supportive of our other findings reported elsewhere (Berth & Dautzenberg, 2000) according to which the DA has no discernible effect on the chain conformation (sufficiently high ionic strength provided).

Acknowledgements

G.B. thanks the Deutsche Forschungsgemeinschaft (DFG) and the Wella AG, Germany, for financial support and interest. She thanks also Professor Markus Antonietti for giving her the opportunity to do her part of this work at the MPI for Colloids and Interface Research. H.C. acknowledges the Dr. Herrmann Schnell foundation for financial support.

References

Berth, G., & Dautzenberg, H. (1998). Solution behaviour of some selected

polysaccharides studied preferentially by static light scattering. *Recent Research Developments in Macromolecular Research*, *3*, 225–248.

Berth, G., & Dautzenberg, H. (2000). *The degree of acetylation and its effect on the conformation of chitosans in aqueous solution*. submitted for publication.

Berth, G., Dautzenberg, H., & Peter, M. G. (1997). Physico-chemical characterisation of chitosan in dilute solution. *Advances in Chitin Science*, *2*, 429–436.

Berth, G., Dautzenberg, H., & Peter, M. G. (1998). Physico-chemical characterisation of chitosans varying in degree of acetylation. *Carbohydrate Polymers*, *36*, 205–216.

Cölfen, H., & Harding, S. E. (1997). MSTARA and MSTARI: interactive PC algorithms for simple, model independent evaluation of sedimentation equilibrium data. *European Biophysics Journal*, *25*, 333–346.

Elias, H. G. (1990). *Makromoleküle*, Vol 1, Grundlagen: Struktur–Synthese–Eigenschaften. Basel: Hüthig and Wepf Verlag.

Errington, N., Harding, S. E., Vårum, K. M., & Illum, L. (1993). Hydrodynamic characterisation of chitosans varying in degree of acetylation. *International Journal of Biological Macromolecules*, *15*, 113–117.

Harding, S. E. (1981). A compound hydrodynamics shape function derived from viscosity and molecular covolume measurements. *International Journal of Biological Macromolecules*, *3*, 340–341.

Harding, S. E. (1995). On the hydrodynamic analysis of macromolecular conformation. *Biophysical Chemistry*, *55*, 69–93.

Harding, S. E., & Cölfen, H. (1995). Inversion formulae for ellipsoid of revolution macromolecular shape functions. *Analytical Biochemistry*, *228*, 131–142.

Harding, S. E., Horton, J. C., & Cölfen, H. (1997a). The E. L. L. I. P. S. suite of macromolecular conformation algorithms. *European Biophysics Journal*, *25*, 347–359.

Harding, S. E., Day, K., Dhami, R., & Lowe, P. M. (1997b). Further observations on the size, shape and hydration of kappa-carrageenan in dilute solution. *Carbohydrate Polymers*, *32*, 81–87.

Lavrenko, P. N., Linow, K. J., & Görnitz, E. (1992). The concentration dependence of the sedimentation coefficient of some polysaccharides in very dilute solution. In S. E. Harding, A. J. Rowe & J. C. Horton, *Analytical ultracentrifugation in biochemistry and polymer science* (pp. 517–531). Cambridge: The Royal Society (chap. 28).

Ottøy, M. H., Vårum, K. M., Christensen, B. E., Anthonsen, M. W., & Smidsrød, O. (1996). Preparative and analytical size-exclusion chromatography of chitosans. *Carbohydrate Polymers*, *31*, 253–261.

Pavlov, G. M., & Selyunin, S. G. (1986). Speed sedimentation, molecular mass and conformational parameters of some soluble chitin derivatives. *Vysokomolekulyarnye Soedineniya, Ser. A*, 1727–1731.

Pavlov, G. M., Korneeva, E. V., Harding, S. E., & Vichoreva, G. A. (1998). Dilute solution properties of carboxymethylchitins in high ionic strength solvent. *Polymer*, *39*, 6951–6961.

Perrin, F. (1936). Movement Brownian d'un ellipsoide II. Translation et diffusion de molecules ellipsoidales. Rotation libre et depolarisation des fluorescences. *Journal of Physique Radium*, *7*, 1–11.

Rowe, A. J. (1977). Concentration-dependence of transport processes — general description applicable to sedimentation, translational diffusion and viscosity coefficients of macromolecular solutes. *Biopolymers*, *16* (12), 2595–2611.

Scheraga, H. A., & Mandelkern, L. (1953). Consideration of hydrodynamic properties of proteins. *Journal of the American Chemical Society*, *75*, 179–184.

Simha, R. (1940). The influence of Brownian motion on the viscosity of solutions. *Journal of Physical Chemistry*, *44*, 25–34.

Svedberg, T., & Pedersen, K. O. (1940). *The ultracentrifuge*, Oxford: Clarendon Press.

Tanford, Ch. (1965). *Physical chemistry of macromolecules*. (3rd ed.) New York: Wiley.

Tsaih, M. L., & Chen, R. H. (1999). Effects of ionic strength and pH on the diffusion coefficients of chitosan molecules in solution. *Journal of Applied Polymer Science*, *73*, 2041–2050.

Vanneste, K., Slootmaekers, D., & Reynaers, H. (1996). Light scattering studies of the dilute solution behaviour of kappa-, iota- and lambda-carrageenan. *Food Hydrocolloids*, *10*, 99–107.

Wales, M., & van Holde, K. E. (1954). The concentration dependence of the sedimentation constants of flexible macromolecules. *Journal of Polymer Science*, *14*, 81–86.

Wu, C., Zhou, S., & Wang, W. (1995). A dynamic laser light-scattering study of chitosan in aqueous solution. *Biopolymers*, *35*, 385–392.

Yamakawa, H. (1971). *Modern theory of polymer solutions*, New York: Harper and Row.